




Paper Type: Original Article

Dynamic Response of Waves on a Non-Homogeneous Impedance Solid with Variable Amplitudes of Corrugated Surface under a Magnetic Field

Augustine Igwebuike Anya* 

Department of Mathematical Sciences, Faculty of Natural and Applied Sciences, Veritas University Abuja, Bwari-Abuja, Nigeria; anyaa@veritas.edu.ng; anyaaugustineigwebuike@gmail.com.

Citation:

Received: 10 July 2025

Revised: 16 October 2025

Accepted: 07 November 2025

Any, I. A. (2025). Dynamic response of waves on a non-homogeneous impedance solid with variable amplitudes of corrugated surface under a magnetic field. *Annals of process engineering and management*, 2(4), 269-285.

Abstract


In this investigation, a solution model is proposed to characterize and analyze the stresses and displacements induced by surface waves in a corrugated, inhomogeneous, fibre-reinforced material under magneto-elastic influences, with some underlying mechanical inclinations. The governing equations of the model problem are presented using the material's constitutive relations. By the normal mode method, we derived the analytical solution of the model whilst utilizing non-dimensionalization of the equations of motion to reduce redundant parameters, and so on. Also, the model considers only a case in which the boundary corrugation or wavy-like phenomenon has various amplitudes and inhomogeneous impedance conditions, resulting in a complex geometry. Following this, suitable applications of the formulated boundary conditions – variable-amplitude corrugation and inhomogeneous impedance conditions, along with mechanical inclinations - are used to ensure that the complete solutions for the wave's stresses and displacements in the inhomogeneous medium are derived. In addition, the distributions of stresses and displacements in these fields are graphically presented using MATHEMATICA software to assess the variations and behaviors of the considered physical quantities, including the nonlocal parameter, variable-amplitude corrugation, inhomogeneous impedance parameters, and angles of inclination. We observe that these parameters significantly affect the distribution of the surface wave across the material, with the nonlocal, angle-of-inclination, and inhomogeneous parameters causing downward trends in the distribution profiles as they increase. Exceptional cases of constant amplitude can be obtained from our model if we neglect one of the quantities with variable amplitude in the corrugation and the magnetic impact on the medium. This study should prove helpful for examinations in geophysics and seismology, where the analysis of surface disturbances is required.

Keywords: Variable amplitudes of corrugation, Magnetic influence, Inhomogeneous impedance boundaries, Inhomogeneous medium, Angles of inclination, Wavenumber.

1 | Introduction

In the field of solid mechanics, investigations on wave propagations in and on surfaces of materials are still much paramount as a result of the roles played by these waves in our everyday activities especially in the industries. And the nature of materials (whether naturally or artificially engineered) in which they travel is also

 Corresponding Author: anyaa@veritas.edu.ng, anyaaugustineigwebuike@gmail.com

 <https://doi.org/10.48314/apem.vi.50>



Licensee System Analytics. This article is an open-access article distributed under the terms and conditions of the Creative Commons Attribution (CC BY) license (<http://creativecommons.org/licenses/by/4.0>).

of great concern to scientists since this helps for materials characterizations, design, and manufacturing. Moreover, the nature of waves that propagates primarily on materials surfaces could be in the form of Rayleigh, Stoneley and Love types of surface waves. These gives great credence in furthering examinations likened to their displacements and stresses which they exerts in the course of their propagations across surfaces of materials. Owing to this and material characteristics which greatly influences wave propagations, researchers in this field tend to focus their investigations hugely on either of the two classifications of materials- Isotropic or Anisotropic material. Composite materials are in the class of anisotropic materials. These composites such as the fibre-reinforced composites gives good quality when utilized in several applications of engineering and geophysical works due to its flexibility, malleability and even tensile strength. Thus, in other to gain insights about the movements of these surface waves on composite materials, we sometimes employ mathematical models and its solutions. This was demonstrated in one of the researches conducted by Spencer [1], where he gave account of deformations occasioned by fibre-reinforced composites in classical theories. However, investigations of waves on surfaces of materials can still occur using the non-local theory of elasticity, Barak et al. [2] which involves incorporating the product of the squared of both the internal friction and material constants to the equations of motion and thereby introducing higher order gradients in the dynamical equations of the wave.

Furthermore, when deformations of homogeneous materials occurs in the mathematical sense, it creeps in inhomogeneity in the equations of motion defining the wave phenomena as a result of change in state of the material constants. These are usually expressed in either of decaying or growing exponential functions of the material constants along a coordinate of interest, through which waves are analyzed, Barak et al. [3]. Aside the nonlocal theory of wave considerations on composites, without further incorporations of some environmental, mechanical and even electrical factors into the model problems, scientists may not accurately predict the exhibitions of the phenomena occasioned by surface waves on materials. Hence, such factors used like the mechanical impedance, Singh [4] and imperfect (corrugated) boundaries, Asano [5] helps to accommodate analysis of waves across and along interfaces of materials where complex dynamics are involved-since most materials are not planar in nature.

In addition, authors have strived to employ other physical factors that affects wave modulations coupled with inhomogeneity, non-locality and impedance-corrugated boundaries in furthering the course of wave propagation and material behaviors upon the action of say, stress. Singh et al. [6]–[8] proposed and investigated on qP-wave where the interface is corrugated and having two different initial stress on an elastic solid, impacts of corrugated surfaces reinforcement, hydrostatic stress, inhomogeneity and anisotropy on Love waves and also on the influences of loose bonding and sinusoidal boundary conditions on Rayleigh wave propagation on material surfaces. Das et al. [9] conducted studies that involves waves on a non-homogeneous elastic solid with gravity effects Also, Abd-Alla et al. [10] opined the impact of rotation and inhomogeneity on an infinite cylinder of orthotropic elastic material with magnetic impacts whilst Chattopadhyay et al. [11] examined dispersion of Love-type of wave by utilizing non-planar conditions in the thickness of a heterogeneous solid half-space. Roy et al. [12] dealt with studies to depicted propagation and reflection of plane waves with effects of rotation, magnetism and surface stress on a fibre-reinforced material. Subsequently, Singh et al. [13]; Gupta et al. [14]; Anya et al. [15]–[18] went further to make investigations linked to magnetic effects on surface waves in a rotating inhomogeneous solid having corrugated-impedance conditions, and non-local impacts, respectively. Likewise, Maleki and Jafarzadeh [19] investigation lied on the determination of the influences of various geometrical aspects on horizontal impedance which are consider useful when treating surface waves on materials and their counterpart Chowdhury et al. [20] went ahead to propound the dispersion of Stoneley waves on an imperfect interface of double hydrostatic stressed MTI media while Singh and Kaur [21], [22] engineered a solution on Rayleigh surface wave at an impedance boundary of an incompressible micropolar elasticity and orthotropic solid. In a similar vein, Sahu et al. [23] conducted a Mathematical analysis of Rayleigh waves on a non-planar boundary for two different materials. Giovannini [24] developed theory associated with dipole-exchange spin-wave propagation in periodically corrugated films while Rakshit et al. [25], [26] went further to examine stress for the imperfect surface of

visco-porous piezoelectric half-space with moving load. Eringen [27], [28] opined models to account for linear theory of non-local elasticity and dispersion of plane waves and nonlocal continua. Thus, the investigations occasioned by Rayleigh wave in a rotating nonlocal magneto-elasticity on a solid half-space were carried out by Roy et al. [29]. While Said et al. [30] developed and demonstrated that the impact of initial stress and rotation on a nonlocal fiber-reinforced thermo-elastic medium with a fractional derivative heat transfer is feasible. Now, all the examined body of knowledge posited above concentrated their studies either in part or individual investigations of the physical interacting parameters with the material make-up, in order to propound a model and its analysis for various surface waves that exerts on materials. They do not account for the analysis of displacements and stresses when variable amplitudes of corrugation-impedance, inhomogeneous conditions and magnetic field theory on the solid medium impacts.

In the light of the foregoing and the literatures given above, this work envisages a surface wave solution through mathematical modelling and analysis of the displacements, normal and shear stresses on an inhomogeneous material. The derivations of the analytical solutions of the displacements and stresses of the waves on the solid material are achieved by incorporating magnetic influences, non-uniform amplitudes of corrugation, mechanical inclination of the medium and inhomogeneous impedance conditions in the model problem. Upon derivations of the analytical solutions through normal mode principle, we graphically depict using MATHEMATICA software, the various effects of the contributing physical parameters magnetic field, mechanical inclination, variable amplitudes of corrugations, impedance and inhomogeneity on the displacements and stresses of the surface waves on the solid medium. We observe that these contributing physical parameters have considerable amount of impacts on the solid and in turn the displacements and stresses of the wave on the material. Thus, deductions were made such that increase in the angle of inclination, inhomogeneity, and wavenumber results to decrease on the displacements and stresses of the wave on the inhomogeneous material whilst noting uniform characteristics along extended length of the normal coordinate of space coordinate - probably due to reinforcement and considered quantities on the material.

2 | The Mathematical Model and Formulations

Following Spencer and [1] Anya et al. [31], [32], the mathematical formulation of the model through presentation of the fields' quantities incorporated in the stress-strain constitutive equation for a corrugated homogeneous fibre-reinforced solid half-space is stated:

$$\sigma_{ij} = \lambda \varepsilon_{kk} \delta_{ij} + 2\mu_T \varepsilon_{ij} + \alpha(q_k q_m \varepsilon_{km} \delta_{ij} + \varepsilon_{kk} q_i q_j) + 2(\mu_L - \mu_T)(q_i q_k \varepsilon_{kj} + q_j q_k \varepsilon_{ki}) + \beta(q_k q_m \varepsilon_{km} q_i q_j), \quad i, j = k = m = 1, 2, 3, \quad (1)$$

Eq. (1) holds true when λ is the Lame's constant, σ_{ij} the stress tensor, ε_{ij} the strain tensor, u_i the displacement vector, δ_{ij} denotes the Kronecker-delta function, and $(\alpha, \beta, (\mu_L - \mu_T))$ the fiber-reinforced parameters. Mathematically, we represent the strain- $\varepsilon_{ij} = \frac{1}{2}(u_{i,j} + u_{j,i})$. We choose $\vec{q} = (r_1, r_2, r_3)$ such that $\vec{q} = (1, 0, 0)$ gives the directions of the fibre reinforcement employed in the model problem. Thus, the governing equations of motion incorporating magnetic field theory for the homogeneous fibre-reinforced solid are given below.

$$\sigma_{ij,j} + F_i = \rho \ddot{u}_i, \quad (2)$$

where $F_i = \mu_0 H_0^2 (e_{,i} - \varepsilon_0 \mu_0 \ddot{u}_i, e_{,2} - \varepsilon_0 \mu_0 \ddot{u}_2, 0) = (F_1, F_2, F_3), i = 1, 2, 3$, $H_i = H_0 \delta_{i3} + h_i$, $h_i = (0, 0, -e)$, is induced magnetic field, $e = u_{i,i}, i = 1, 2$, ε_0 is the electric permeability. The material is assumed to be in the $x_1 x_2$ - plane. $h_i(x_1, x_2, x_3) = -u_{k,k} \delta_{i3}$. $h_i(x_1, x_2, x_3) = -u_{k,k} \delta_{i3}$. H_i is the magnetic vector field, and μ_0 is the magnetic permeability according to Maxwell's theory. Also, recall that Einstein's summation convention was used throughout this write-up. And where the index after the comma is, entails partial derivatives with respect to the coordinate, and superscript dot means partial derivative with respect to time. Since we are dealing with inhomogeneity in the medium, it is sufficient to introduce exponentially decaying material parameters due to

the deformations as the wave propagates through the solid. Following Khan et al. [33] and Sethi et al. [34], this can be represented as: $\beta = \beta_0 e^{-mx_2}$, $\lambda = \lambda_0 e^{-mx_2}$, $\alpha = \alpha_0 e^{-mx_2}$, $\mu_L = \mu_{L0} e^{-mx_2}$ and $\rho = \rho_0 e^{-mx_2}$, $\mu_T = \mu_{T0} e^{-mx_2}$. Here, m is the inhomogeneity of the fibre-reinforced solid half-space. When $m=0$, we recover the homogeneous nature of the material.

Now, if we make considerations by introducing the inhomogeneous quantity into *Eqs. (1) and (2)*, and the magnetic components, we get the components of the dynamic equations of the wave:

$$(\lambda + 2\alpha + 4\mu_L - 2\mu_T + \beta + \mu_0 H_0^2)u_{1,11} + (\alpha + \lambda + \mu_L + \mu_0 H_0^2)u_{2,21} + \mu_L u_{1,22} - m\mu_T(u_{1,2} + u_{2,1}) = \{\rho + \varepsilon_0 \mu_0^2 H_0^2\} \ddot{u}_1. \quad (3)$$

$$(\alpha + \lambda + \mu_L + \mu_0 H_0^2)u_{1,12} + \mu_L u_{2,11} + (\lambda + 2\mu_T + \mu_0 H_0^2)u_{2,22} - m(\lambda + \alpha)u_{1,1} - m(\lambda + 2\mu_T)u_{2,2} = \{\rho + \varepsilon_0 \mu_0^2 H_0^2\} \ddot{u}_2. \quad (4)$$

$$\mu_L u_{3,11} + \mu_T u_{3,22} - m\mu_T u_{3,2} = \rho \ddot{u}_3. \quad (5)$$

However, we can put all the equations above, that is, *Eqs. (3)–(5)* in the form below:

$$Q_1 u_{1,11} + Q_2 u_{2,21} + Q_3 u_{1,22} - mQ_4(u_{1,2} + u_{2,1}) = \{\rho + \varepsilon_0 \mu_0^2 H_0^2\} \ddot{u}_1. \quad (6)$$

$$Q_2 u_{1,12} + Q_3 u_{2,11} + Q_5 u_{2,22} - mQ_6 u_{1,1} - mQ_7 u_{2,2} = \{\rho + \varepsilon_0 \mu_0^2 H_0^2\} \ddot{u}_2. \quad (7)$$

$$Q_3 u_{3,11} + Q_4 u_{3,22} - mQ_4 u_{3,2} = \rho \ddot{u}_3. \quad (8)$$

Such that $Q_1 = (\lambda + 2\alpha + 4\mu_L - 2\mu_T + \beta + \mu_0 H_0^2)$, $Q_2 = (\alpha + \lambda + \mu_L + \mu_0 H_0^2)$, $Q_3 = \mu_L$, $Q_4 = \mu_T$,

$Q_5 = (\lambda + 2\mu_T + \mu_0 H_0^2)$, $Q_6 = (\lambda + \alpha)$, $Q_7 = (\lambda + 2\mu_T)$. When m is considered to be zero into *Eqs. (6)–(8)*, that is, $m=0$, the dynamic equations of the wave are recovered for a homogeneous material. Now, let us utilize the following dimensionless parameters: $(x'_1, x'_2, u'_1, u'_2, \kappa') = c_0(x_1, x_2, u_1, u_2, \kappa)$,

$c_0^2 = Q_1 / \rho$, $(t') = c_0^2 t$, $\sigma'_{ij} = \sigma_{ij} / \rho c_0^2$, and put them into *Eqs. (6)–(8)* and afterwards dropping the sign “'” from the resulting equations, a nondimensionalized equation of motion is thus presented below:

$$u_{1,11} + Q_{12} u_{2,21} + Q_{13} u_{1,22} - mQ_{24}(u_{1,2} + u_{2,1}) = \{1 + \varepsilon_0 \mu_0^2 H_0^2 / \rho\} \ddot{u}_1. \quad (9)$$

$$Q_{12} u_{1,12} + Q_{13} u_{2,11} + Q_{15} u_{2,22} - mQ_{26} u_{1,1} - mQ_{27} u_{2,2} = \{1 + \varepsilon_0 \mu_0^2 H_0^2 / \rho\} \ddot{u}_2. \quad (10)$$

$$Q_{13} u_{3,11} + Q_{14} u_{3,22} - mQ_{24} u_{3,2} = \ddot{u}_3. \quad (11)$$

$$(Q_{12}, Q_{13}, Q_{14}, Q_{15}, Q_{16}, Q_{17}) = ((Q_2, Q_3, Q_4, Q_5, Q_6, Q_7) / Q_1),$$

$$(Q_{24}, Q_{26}, Q_{27}) = (Q_{14}, Q_{16}, Q_{17}) \rho^{1/2} / Q_1^{3/2}.$$

3 | Normal Mode Analysis

This section allows us to employ in the equations of motion, the harmonic solution approach, otherwise called the eigenvalue method associated with wave analysis, to formulate and derive the analytical solution of the displacements, which in turn would lead to the derivations of the stresses on the nonlocal inhomogeneous impedance solid with variable amplitudes and mechanical inclinations with magnetic effects. On application of this assumption, we can state that the components of the horizontal and normal displacements assume the form below:

$$u_i = (\bar{u}_i(x_2)) e^{i\omega t + i b x_1}, i = 1, 2. \quad (12)$$

Applying *Eq. (12)* to the *Eqs. (9)–(11)*, we have the three ODEs below, which lie in the direction of the normal coordinate of space x_2 :

$$(Q_{13} D^2 - mQ_{24} D - b^2 - K) \hat{u}_1 + (iQ_{12} b D - mQ_{24} b i - 2\rho\Omega\omega) \hat{u}_2 = 0. \quad (13)$$

$$(iQ_{12} b D - mbiQ_{26} + 2\rho\Omega\omega) \hat{u}_1 + (Q_{15} D^2 - mQ_{27} D - Q_{13} b^2 - K) \hat{u}_2 = 0. \quad (14)$$

$$(Q_{14} D^2 - mQ_{24} D - (Q_{13} b^2 + \omega^2) \hat{u}_3 = 0. \quad (15)$$

Where $K = (1 + \epsilon_0 \mu_0^2 H_0^2 / \rho) \omega^2$ and in Eqs. (13)–(15) gives second-order ODEs in the direction of x_2 coordinate of space. Now, observe that Eqs. (13) and (14) are coupled while Eq. (15) is not. Since we are interested in a 2-D analysis, that is, analysis in the plane of x_1, x_2 , it behooves us to take non-trivial solutions of Eqs. (13) and (14) which would give the quartic Eq. (16):

$$(q_{11} D^4 + q_{12} D^3 + q_{13} D^2 + q_{14} D + q_{15}) (\hat{u}_1, \hat{u}_2) = 0. \quad (16)$$

The polynomial equation in D in Eq. (16) has complex coefficients $q_{ii}, i = 1, 2, 3, 4, 5$ (Appendix given) which are characterized in terms of the constants of the considered material. Owing to this, assumptions are made such that $\eta_i, i = 1, 2, 3, 4$ the real positive roots of Eq. (16) and also, by the presumptions already established for the use of normal mode solution analysis above of the normal mode approach, \hat{u}_1, \hat{u}_2 can be formulated and presented as follows:

$$(\hat{u}_1, \hat{u}_2) = (S_n, S_{1n}) e^{-\eta_n x_2} \quad n = 1, 2, 3, 4. \quad (17)$$

Furthermore, the quantities S_n and S_{1n} in Eq. (17) are functions of the wavenumber b that lies in the direction of the horizontal coordinate of space, and ω as the complex frequency of the waves' propagation on the surfaces of the material. Making use of Eq. (17) in Eqs. (13) and (14), the relation for S_{1n} given in terms of S_n follows:

$$S_{1n} = N_{1n} S_n. \quad (18)$$

$$N_{1n} = h_{1n} / h_{2n}, \quad h_{1n} = (Q_{13} \eta_n^2 + mQ_{24} \eta_n - b^2 - K + (iQ_{12} b \eta_n + mbiQ_{26})).$$

$$h_{2n} = (Q_{15} \eta_n^2 - Q_{13} b^2 + mQ_{27} \eta_n - K + (iQ_{12} b \eta_n + mbiQ_{24})). \quad n = 1, 2, 3, 4.$$

Owing to this, we derive and present the total components of displacements (horizontal and normal displacements) and normal and shear stresses occasioned by the surface wave on the material:

$$u_1 = S_n e^{-\eta_n x_2 + \omega t + ibx_1}, \quad u_2 = N_{1n} S_n e^{-\eta_n x_2 + \omega t + ibx_1},$$

$$\tau_{11} = \{ib(1 - (\mu_0 H_0^2 / Q_1)) - \eta_n N_{1n} N_{16}\} S_n e^{-(\eta_n + m)x_2 + \omega t + ibx_1},$$

$$\sigma_{22} = \{ibQ_{16} - \eta_n N_{1n} Q_{17}\} S_n e^{-(\eta_n + m)x_2 + \omega t + ibx_1}, \quad \sigma_{12} = (ibN_{1n} - \eta_n) Q_{13} S_n e^{-(\eta_n + m)x_2 + \omega t + ibx_1}$$

$$\sigma_{21} = (ibN_{1n} - \eta_n) Q_{13} S_n e^{-(\eta_n + m)x_2 + \omega t + ibx_1}. \quad n = 1, 2, 3, 4.$$

4 | Inhomogeneous Impedance and Variable Amplitudes of Corrugation Mechanical Inclination

In this section, we need to establish the nature of corrugation to be utilized in our model. However, following Asano [5], we reformulated $x_2 = \xi(x_1)$ and $\xi(x_1) = \xi_1 e^{ibx_1} + \xi_{-1} e^{-ibx_1}, 1 = 1, 2, 3, 4, \dots$ such that the variability of the amplitudes of corrugation could suffice. That is $\bar{\xi}(x_1) = \bar{\xi}_1 e^{ibx_1} + \bar{\xi}_{-1} e^{-ibx_1}, 1 = 1, 2, 3, 4, \dots$, such that we define $\bar{\xi}_1^\pm = (a + cx_1) / 2$, and $\bar{\xi}_1^\pm = (F_1 + I_1) / 2, 1 = 2, 3, \dots$ imply $\bar{\xi}(x_1) = (a + cx_1) \cos bx_1 + F_2 \cos 2bx_1 + I_2 \sin 2bx_1 + \dots + F_l \cos lbx_1 + I_l \sin lbx_1$. Here, ξ_1 and ξ_{-1} entails the Fourier expansion coefficients and l is the series expansion order. a connotes the uniform amplitude of corrugation and b the wavenumber with wavelength $2\pi / b$ for the Asano [5] model and π / b for the current model under investigation, such that when $c = 0$, we recover the Asano [5] model of constant amplitude of

corrugation. This means $\bar{\xi}(x_1) = (a + cx_1)\cos bx_1$ that the variable corrugation of the current model and $(a + cx_1)$ the non-uniform amplitudes of corrugation, and $\xi(x_1) = a \cos bx_1$ as the model of corrugation with constant amplitude a Asano [5]. We illustrate two of these cases graphically as given in Fig. 1.

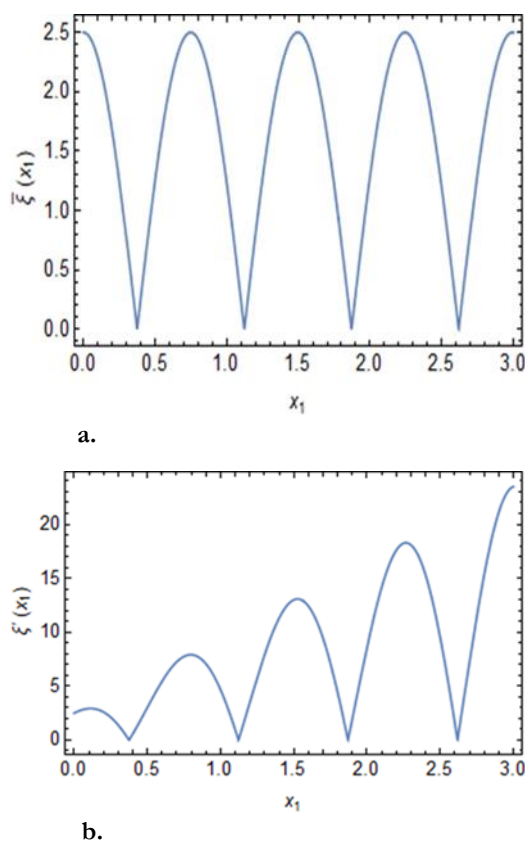


Fig. 1. a. Illustration of constant amplitude of corrugation Asano [5] and b. illustration of variable amplitude of corrugation, for all x_1 .

Thus, taking into account the variable amplitudes of corrugation and the inhomogeneous boundary conditions, we have: 1) $u_1 = 0$, $u_2 = 0$, at $x_2 = \bar{\xi}(x_1)$, for all x_1 and t , 2) Normal stress w.r.t $x_2 = \bar{\xi}(x_1)$ yields the following condition: $\sigma_{22} + \bar{\sigma}_{22} - \bar{\xi}'(x_1)\sigma_{21} + \omega\hat{Z}_2 u_2 = -\bar{F}_1 e^{i\omega t + ibx_1} \cos \theta$, for all x_1 and t . Where $\bar{\sigma}_{22} = \mu_0 H_0^2 (u_{1,1} + u_{2,2})$ Anya et al. [31], stipulates additional stress on the material according to Maxwell theory, and 3) conditions on the shear stress follows as: $\sigma_{12} - \bar{\xi}'(x_1)\sigma_{11} + \omega\hat{Z}_1 u_1 = -\bar{F}_1 e^{i\omega t + ibx_1} \sin \theta$, $\forall x_1$ and t , Anya et al. [31], [32] and Azhar et al. [35]. Here, the parameters for inhomogeneity of the impedance are denoted as \hat{Z}_1 and \hat{Z}_2 Anya et al. [31], [32] and Ailawalia et al. [36]. Since we are formulating an inhomogeneous impedance at the boundary, it suffices to consider $\hat{Z}_1, \hat{Z}_2, \bar{F}_1$ such that $(\hat{Z}_1, \hat{Z}_2, \bar{F}_1) = (Z_1, Z_2, F_0) e^{-mx_2}$ where Z_1, Z_2, F_0 are considered homogeneous in their own merit. This means that we can achieve Z_1 , and Z_2 and F_1 , by recovering them when $m=0$. Moreover, these propositions stipulate the four equations of inhomogeneous impedance boundary condition in a non-homogeneous corrugated solid given below.

$$S_n = 0. \quad (19)$$

$$N_{1n} S_n = 0. \quad (20)$$

$$\{ibQ_{16} - \eta_n N_{1n} Q_{17}\} e^{-(\eta_n)\xi(x_1)} S_n + [(a + cx_1)b \sin bx_1 - c \cos bx_1] \{(ibN_{1n} - \eta_n)Q_{13}\} e^{-(\eta_n)\xi(x_1)} S_n + \{\omega N_{1n} Z_2 + \mu_0 H_0^2 (ib - \eta_n N_{1n})\} e^{-(\eta_n)\xi(x_1)} S_n = -F_0 \cos \theta. \quad (21)$$

$$\begin{aligned} & \{ \{ibN_{in} - \eta_n\} Q_{13} S_n + [(a + cx_1)b \sin bx_1 - c \cos bx_1] \{ib(1 - (\mu_0 H_0^2 / Q_1)) - \eta_n N_{in} Q_{16}\} S_n \\ & + \{\omega Z_1\} S_n e^{-(\eta_n)\xi(x_1)} = -F_0 \sin \theta, n = 1, 2, 3, 4. \end{aligned} \quad (22)$$

Hence, finding the solutions of the algebraic systems of 4x4 equations (Eqs. (19)–(22)) for S_n , $n = 1, 2, 3, 4$, we derive the closed-form results of the displacements and stresses occasioned by the surface waves on the corrugated inhomogeneous magneto-elastic solid inclined at angle θ with inhomogeneous impedance conditions. We also note that when one of the variable amplitude parameters, say, $c = 0$, the distributions of stresses and the displacements become undoubtedly a special case of the Asano [5] model found in the literature for corrugation, where uniform amplitude of corrugation holds on the material.

5 | Numerical Results and Discussion

To visualize the derived closed-form solutions of the displacements and stresses occasioned by the surface wave on the solid medium, we have plotted the displacements and stresses of the wave on the material as a function of the normal coordinate x_2 of space by using the material constants Othman et al. [37] and other parameters as given below. This is to examine the effects of the considered physical parameters — magnetic field, mechanical inclination, variable corrugation amplitudes, and inhomogeneous parameters — on the wave's displacements and stresses in the inhomogeneous solid half-space. See Figs. (2)–(10) below:

$$\begin{aligned} & \lambda = 3.76 \times 10^9 \text{ kg m}^{-1} \text{ s}^{-2}; \mu_L = 7.86 \times 10^9 \text{ kg m}^{-1} \text{ s}^{-2}; \mu_T = 2.86 \times 10^9 \text{ kg m}^{-1} \text{ s}^{-2}; \rho = 7800 \text{ kg m}^{-3}; \\ & m = 3; Z_1 = 0.54; Z_2 = 0.7; \alpha = -1.78 \times 10^9 \text{ kg m}^{-1} \text{ s}^{-2}; \beta = 2 \times 10^9 \text{ kg m}^{-1} \text{ s}^{-2}; \\ & \omega = (0.8 - 0.5i) \text{ rad / s}; t = 0.2 \text{ s}; b = 4.2; c = 7; \\ & a = 2.5, \kappa = 0.8, F_0 = 0.005 \text{ N}; \theta = 30^\circ. \end{aligned} \quad (17)$$

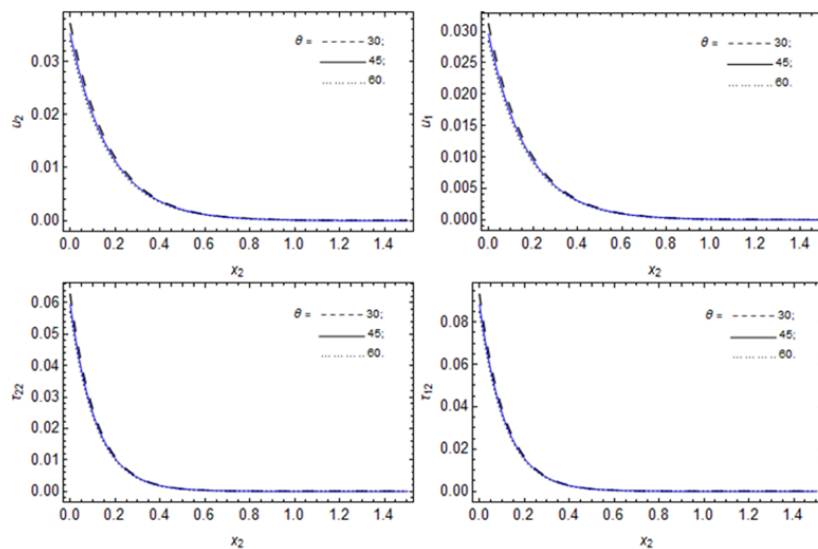


Fig. 2. Distribution of the displacements $u_i, i = 1, 2$ and stresses (τ_{12} and τ_{22}) with respect to x_2 for varying angles of inclination θ in degrees.

Fig. 2 demonstrates the variations of the angles of inclination θ on the displacements $u_i, i = 1, 2$ and stresses (τ_{12} and τ_{22}) of the surface wave on the inhomogeneous material with respect to the normal coordinate x_2 especially when other considered interacting constants of magnetic field, wavenumber b , mechanical inclination F_0 , variable amplitudes of corrugation (a and c) associated with corrugation, impedance $Z_i, i = 1, 2$, and the inhomogeneous m parameters are steady in the system. We note that, in Fig. 2, all the given profiles of wave displacements and stresses exhibited the same behavior. This is such that an upward variation in the angles of inclination results in a decrease in the distribution of the fields' quantities or profiles, whilst

observing uniform trends towards the extended length of the material, and where vanishing effects occur at this instance. This could be due to reinforcement of the material and other interacting physical constants (parameters). Thus, we can infer that a high material inclination angle could reduce surface wave propagation, possibly because the material has low impact, spread, and resistance. We also observed that a low angle of inclination tends to produce a maximum distribution of field profiles near the material's origin.

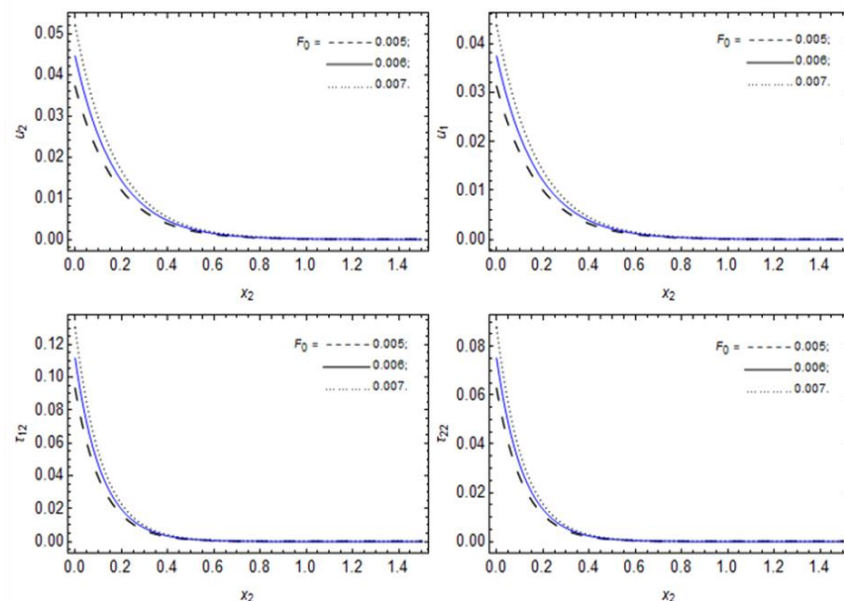


Fig. 3. Distribution of the displacements $u_i, i = 1, 2$ and stresses (τ_{12} and τ_{22}) with respect to x_2 for varying mechanical parameter F_0 associated with inclination.

Also, *Fig. 3* stipulates the effects of the mechanical parameter F_0 associated with the inclination of the medium on the displacements $u_i, i = 1, 2$ and stresses (τ_{12} and τ_{22}) of the surface wave on the inhomogeneous material as against the normal coordinate x_2 . This is so considering when other interacting constants of the magnetic field H_0 , wavenumber b , angle of inclination θ , variable amplitudes (a and c) associated with corrugation, impedance $Z_i, i = 1, 2$, and the inhomogeneous m parameters are held in a fixed state on the material. *Fig. 3* shows that the wave's displacement and stress profiles behave alike. That is, increasing the mechanical parameter leads to a broader distribution of field profiles, whilst observing uniform trends towards an extended material length and the vanishing of effects. Thus, we can infer that a high applied mechanical parameter can increase the propagation of surface waves in the material. This parameter tends to exert a force in terms of a push on the material as a result of this increase, where production of the maxima distributions of the fields' profiles of displacements and stresses occurs, and also close to the origin of the normal coordinate. Near-uniform behavior for this varying mechanical parameter equally occurs in the domain $0.7 \leq x_2 \leq 1.5$.

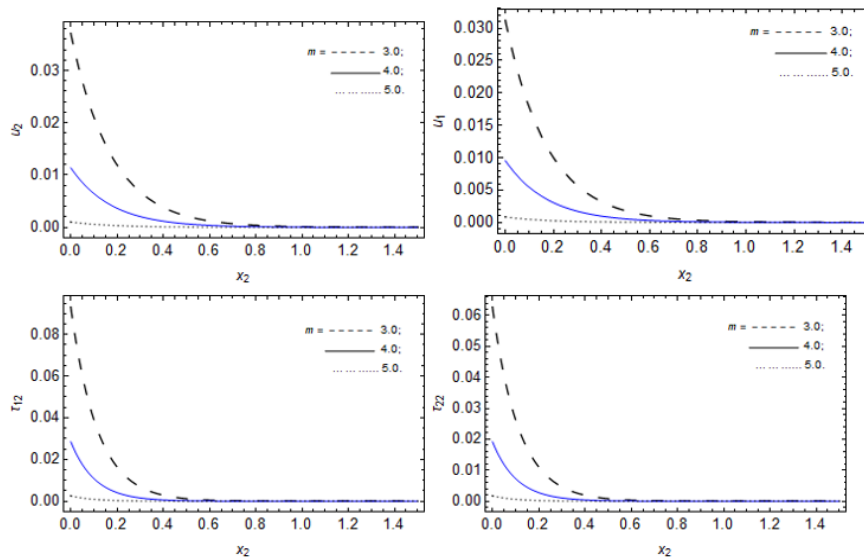


Fig. 4. Distribution of the displacements $u_i, i = 1, 2$ and stresses (τ_{12} and τ_{22}) with respect to for x_2 varying inhomogeneous parameter m .

Subsequently, *Fig. 4* gives the impact of inhomogeneity m of the medium on the displacements $u_i, i = 1, 2$ and stresses (τ_{12} and τ_{22}) against the normal coordinate x_2 of the surface wave on the inhomogeneous material contingent upon other interactions of magnetic field H_0 , wavenumber b , angle of inclination θ , variable (a and c) amplitudes associated with corrugation, impedance $Z_i, i = 1, 2$, and the mechanical parameter F_0 associated with inclination of the medium. We observe that the inhomogeneous quantity m causes a downward trend in the distribution of displacements $u_i, i = 1, 2$ and stresses (τ_{12} and τ_{22}) (and in the material when its variation is on the rise), while noting close uniformity in the domain $1 \leq x_2 \leq 1.5$. In addition, as the material length increases, the profiles of the displacements and stresses in the material reverse, i.e., decrease. Thus, less inhomogeneity of the medium produces maxima profiles of the fields' distributions, especially at $m = 3$ and very close to $x_2 = 0$. the minima values of the distributions of the quantities of displacement and stresses of the wave on the material, which were noticed for high inhomogeneity, i.e., $m = 5$ whilst noting a wide gap in the behavior of these variations in the domain $0 < x_2 < 0.3$.

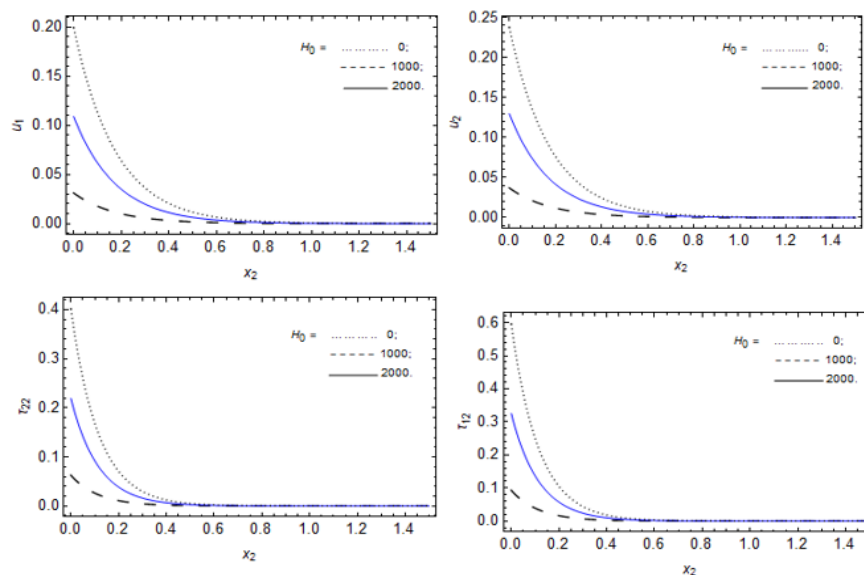


Fig. 5. Distribution of the displacements $u_i, i = 1, 2$ and stresses (τ_{12} and τ_{22}) with respect to x_2 for varying magnetic field H_0 .

Consequently, *Fig. 5* showcases the exhibitions of the magnetic field H_0 of the medium on the displacements $u_i, i = 1, 2$ and stresses (τ_{12} and τ_{22}) of the surface wave on the inhomogeneous half-space with respect to the normal coordinate x_2 . This is achieved if the interaction of inhomogeneity m of the medium, wavenumber b , angle of inclination θ , variable amplitudes (a and c) associated with corrugation, impedance $Z_i, i = 1, 2$, and the mechanical parameter F_0 associated with inclination of the medium are in constant application on the medium. We witness a uniform behavior in distributions of the displacements and stresses at this instance, for $x_2 \geq 1$ and when the magnetic field H_0 increases. Also, an increase in the magnetic field in the medium tends to decrease the distribution of displacements. It stresses in the material, especially along the extended length of the inhomogeneous medium, where the minimum values of the distributions of the field quantities occur. Thus, we deduce that the maximum values of the distributions occur when the magnetic field H_0 is negligible, say, at $H_0 = 0$ and also the length of the normal coordinate is small, accordingly.

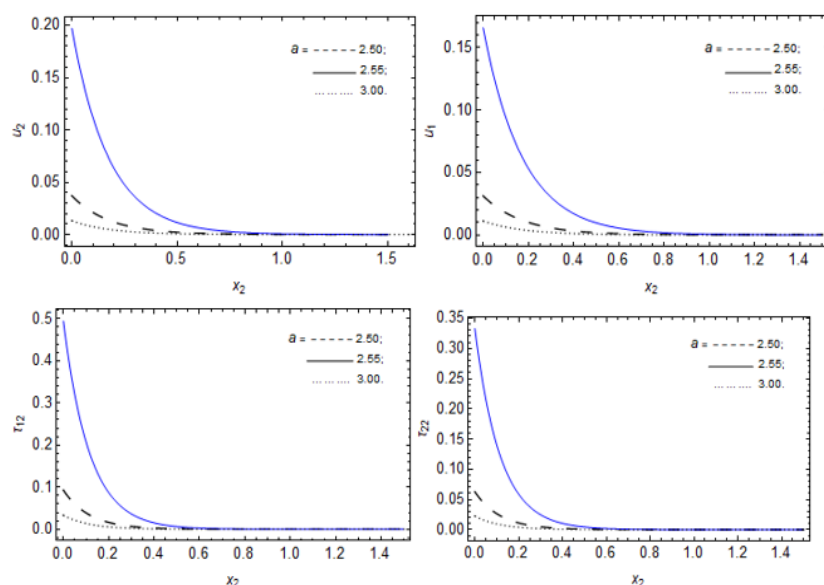


Fig. 6. Distribution of the displacements $u_i, i = 1, 2$ and stresses (τ_{12} and τ_{22}) with respect to x_2 for varying a associated with variable amplitude of corrugation.

More so, *Fig. 6* entails the impacts of one of the parameters a associated with variable amplitudes of corrugation on the displacements $u_i, i = 1, 2$ and stresses (τ_{12} and τ_{22}) of the surface wave on the inhomogeneous half-space with respect to the normal coordinate x_2 . This is actuated such that the interaction of the magnetic field H_0 , inhomogeneity m of the medium, wavenumber b , angle of inclination θ , one of the terms of variable amplitudes c associated with corrugation, impedance $Z_i, i = 1, 2$, and the mechanical parameter F_0 associated with inclination of the medium are fixed on the inhomogeneous medium. We equally observe uniform behaviors in distributions of the displacements and stresses at this instance for $x_2 \geq 1$ when the parameter a associated with variable amplitudes of corrugation increases. Also, an increase in a yields mixed behaviors (in terms of decrease and increase) on the distributions of the displacements and stresses on the material, especially along the extended length of the inhomogeneous medium, where the minimum values of distributions of the fields' quantities of displacements and stresses occur. This decrease is somehow sparsely showcased at this instance within the domain $0 < x_2 < 0.4$. Hence, we adduce that the maxima values of the distributions occur if a is, say, at $a = 2.55$, and the length of the normal coordinate is small, say near $x_2 = 0$.

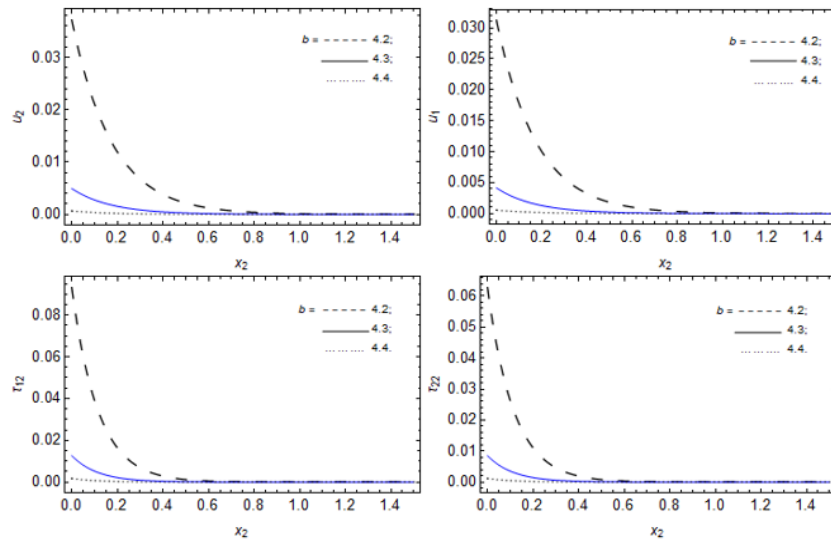


Fig. 7. Distribution of the displacements $u_i, i = 1, 2$ and stresses (τ_{12} and τ_{22}) with respect to x_2 for varying wavenumber b .

Furthermore, *Fig. 7* gives the influence of the wavenumber b on the displacements $u_i, i = 1, 2$ and stresses (τ_{12} and τ_{22}) of the surface wave on the inhomogeneous half-space with respect to the normal coordinate x_2 is depicted. This would only happen when the interaction of the magnetic field H_0 , inhomogeneity m of the medium, angle of inclination θ , terms of variable amplitudes (c, a) associated with corrugation, impedance $Z_i, i = 1, 2$, and the mechanical parameter F_0 associated with inclination of the medium are unchanged on the inhomogeneous fibre-reinforced solid. This indicates that the stress and displacement profiles of the wave in the medium decrease as the wave wavenumber increases. This decrease in profiles is pronounced as the wave propagates from the origin to the extended length of the medium, where not only the minimum values of the distributions occur, but also uniform behaviors in mixed form. Thus, the maxima values of the distributions in *Fig. 7* are given near the origin, say $x_2 = 0$ when the wavenumber b decreases at $b = 4.2$.

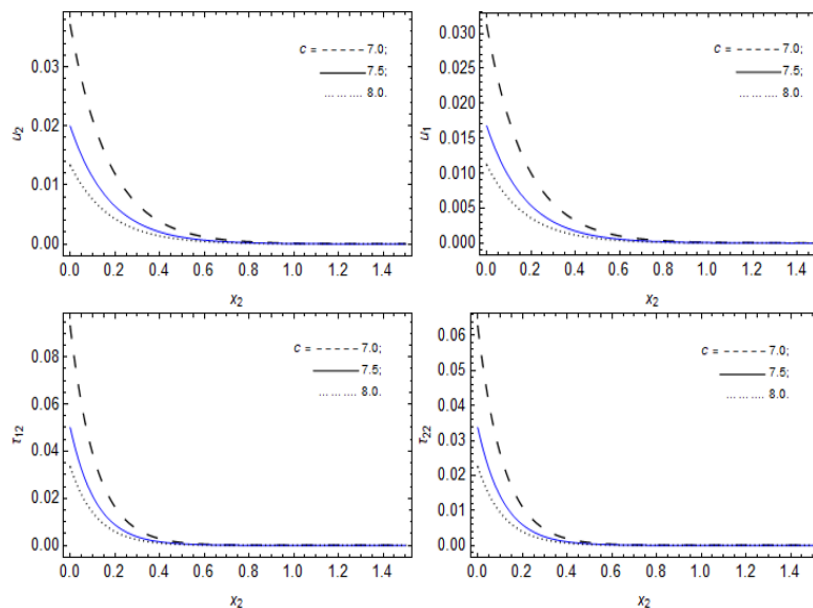


Fig. 8. Distribution of the displacements $u_i, i = 1, 2$ and stresses (τ_{12} and τ_{22}) with respect to x_2 for varying c associated with variable amplitude of corrugation.

Following this, *Fig. 8* depicts the effects of one of the parameters c associated with variable amplitudes of corrugation on the displacements $u_i, i = 1, 2$ and stresses (τ_{12} and τ_{22}) of the surface wave on the inhomogeneous half-space with respect to the normal coordinate x_2 . This is actualized if the interaction of the physical quantities of the magnetic field H_0 , inhomogeneity m of the medium, wavenumber b , angle of inclination θ , one of the terms of variable amplitudes a associated with corrugation, impedance $Z_i, i = 1, 2$, and the mechanical parameter F_0 associated with inclination of the medium are fixed on the inhomogeneous medium. We observe uniform behaviors in distributions of the displacements and stresses at this instance, as $x_2 > 1$ when the parameter c increases. Also, for $x_2 \leq 1$ and considering the increase in stresses and displacements, a decrease in behaviors of the distributions ensues. Hence, we deduce that the maxima values of the distributions occur if c is small, say, at $c = 7$ and the length of the normal coordinate is small, say, close to $x_2 = 0$.

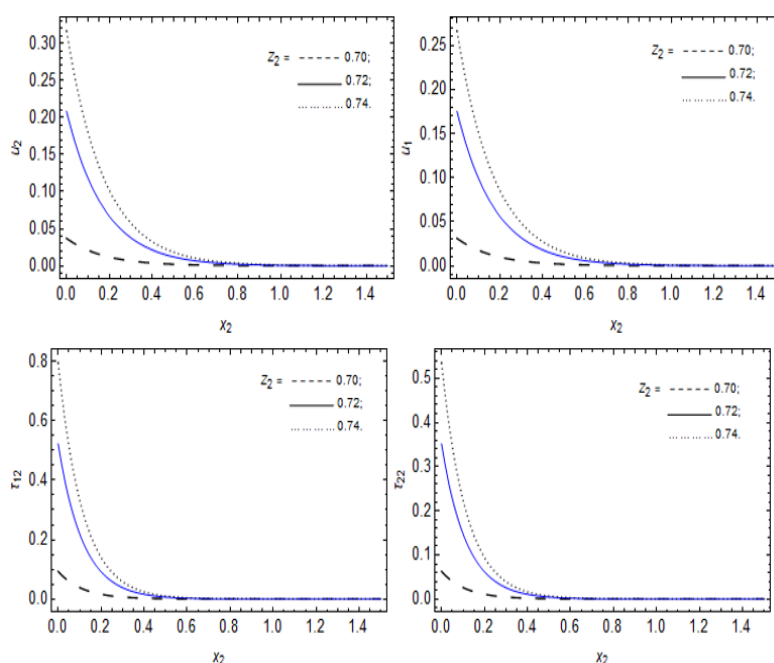


Fig. 9. Distribution of the displacements $u_i, i = 1, 2$ and stresses (τ_{12} and τ_{22}) with respect to x_2 for varying impedance Z_2 .

Furthermore, *Fig. 9* showcases the effects of the normal impedance Z_2 on the displacements $u_i, i = 1, 2$ and stresses (τ_{12} and τ_{22}) of the surface wave on the inhomogeneous half-space with respect to the normal coordinate x_2 of space. This is depicted in such a way that other considered quantities of the model like the magnetic field, wavenumber b , inhomogeneity m of the medium, angle of inclination θ , terms of variable amplitudes (c, a) associated with corrugation, impedance Z_1 , and the mechanical parameter F_0 associated with inclination of the medium, are held in a steady application during the interaction with various Z_2 on the inhomogeneous fibre-reinforce solid. There is no doubt that an increase in the normal impedance on the distributions of displacements and stresses increases the distributions of surface-wave displacements and stresses. In fact, the maximum values of the stresses and displacements occur very close to the origin when the impedance $Z_2 = 0.74$, which is at the highest considered value of variation of Z_2 . However, all distributions tend to decrease along the length of the material and towards the vanishing region, where the minimum values and uniformity occur. However, all distributions tend to decrease along the length of the material and towards the vanishing region, where the minimum values and uniformity occur.

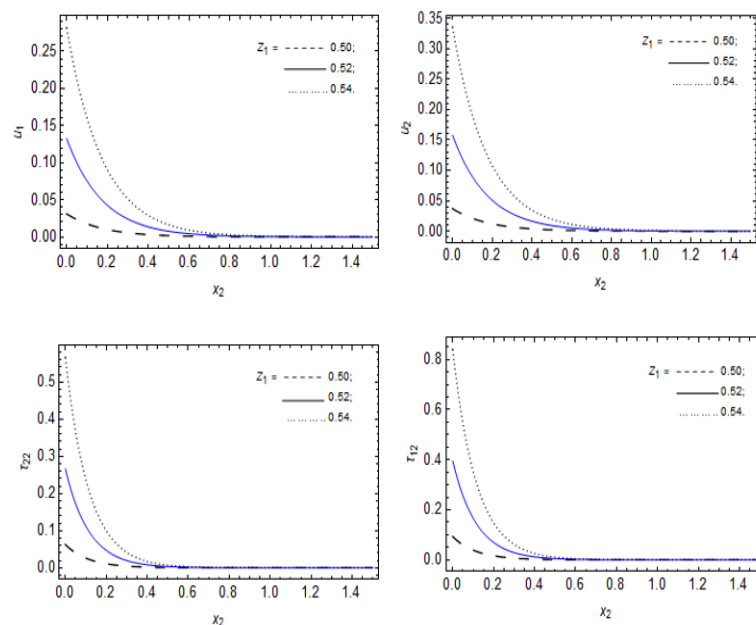


Fig. 10. Distribution of the displacements $u_i, i = 1, 2$ and stresses (τ_{12} and τ_{22}) with respect to x_2 for varying impedance Z_1 .

In a very close analysis, as in *Figs. (9)* and *(10)* also depict the effects of the horizontal impedance Z_1 on the displacements $u_i, i = 1, 2$ and stresses (τ_{12} and τ_{22}) of the surface wave on the inhomogeneous half-space with respect to the normal coordinate x_2 of space. This is demonstrated in such a way that other considered quantities of the model, like the magnetic field, wavenumber b , inhomogeneity m of the medium, angle of inclination θ , terms of variable amplitudes (c, a) associated with corrugation, impedance Z_2 , and the mechanical parameter F_0 associated with inclination of the medium are held in a steady application during the interaction with various Z_1 on the inhomogeneous fibre-reinforced solid. Thus, an increase in the horizontal impedance Z_1 on the distributions of the displacements and stresses increases the behaviour of the distributions of the stresses and displacements of the surface wave. Thus, the maximum values of the stresses and displacements occur very close to the origin when the horizontal impedance $Z_1 = 0.54$, which is the highest considered value of variation of Z_1 . However, all distributions tend to decrease along the length of the material and towards the vanishing region where the minimum values and uniform occurrence exist.

6 | Conclusion

This study explores a mathematical model to aid the analysis of surface wave stresses and displacements in an inhomogeneous fibre-reinforced solid under magneto-elasticity theory, with variable amplitudes of corrugated inhomogeneous impedance and mechanical inclination at the solid's boundary. The constitutive equations of the homogeneous fibre-reinforced medium are considered, and, by deforming the material constants through an exponentially decaying approach, the inhomogeneous governing dynamic equations of motion were derived and presented. Non-dimensionalization of the resulting equations of motion was carried out, and the application of the harmonic solution approach to wave analysis, along with suitable formulations of the variable amplitudes of the corrugated inhomogeneous impedance conditions, aided the derivation of closed-form solutions for the wave displacements and stresses in the inhomogeneous fibre-reinforced material. Computational results in the form of graphical solutions of the derived closed-forms of the stresses and displacements are presented. These graphical solutions thus illustrate the variations and behaviors of the contributing quantities: magnetic field parameter, inhomogeneity of the medium, wavenumber, angle of inclination, terms of variable amplitudes associated with corrugation, impedance, and the mechanical parameter associated with the inclination of the medium, in terms of the displacements and stresses of the surface wave. This is such that:

- I. An increase in the angle of inclination, inhomogeneity, and wavenumber decreases the wave's displacements and stresses in the inhomogeneous material, whilst maintaining uniform characteristics along the extended length of the normal coordinate of space, probably due to reinforcement and the considered quantities in the material.
- II. Also, increasing the magnetic field in the medium leads to increased behavior in the distributions of the wave's stresses and displacements, whilst maintaining uniform behavior along the extended length of the normal coordinate of space.
- III. An increase in the variation of the mechanical parameter F_0 gives a corresponding increase in the displacements and stresses of the wave on the inhomogeneous impedance material.
- IV. One of the variable amplitudes of corrugated parameters a , produces mixed behaviors (in terms of decrease and increase) on the stresses and displacements when increased, while its counterpart c yields a decreasing behavior on the stresses and displacements when increased in some domains of the distributions.
- V. Both the normal and horizontal impedances increase the distribution of the wave's stresses and displacements in the material. Uniform behaviors are also observed along the length of the normal coordinates, indicating the material's resistance to wave motion.

Concisely, this investigation would yield some exceptional cases found in the literature if we take $c = 0$ - leading to formulations of the Asanao [5] model for uniform amplitudes of corrugation. Also, if $a = c = F_0 = 0$ are negligible, results for the classical models in traction-free and planar boundaries are achieved. Thus, we hold that this work would add more information to the research community, especially those working on the analysis of surface waves, geophysical examinations, and mathematics of wave phenomena, where non-homogeneous impedance and variable amplitudes of corrugation with magnetic and mechanical inclination affect the system.

Funding

No funding was received for this study.

Data Availability

The data used in this research were taken from previously published papers, especially the material constants. These are duly cited in the Numerical Results and Discussion section of this manuscript.

Conflicts of Interest

No conflict of interest exists for this submission.

References

- [1] Spencer, A. J. M. (1972). *Deformations of fibre-reinforced materials*. Oxford university press. <https://cir.nii.ac.jp/crid/1970586434862824359>
- [2] Barak, M. S., & Dhankhar, P. (2023). Thermo-mechanical interactions in a rotating nonlocal functionally graded transversely isotropic elastic half-space. *ZAMM-journal of applied mathematics and mechanics zeitschrift für angewandte mathematik und mechanik*, 103(2), e202200319. <https://doi.org/10.1002/zamm.202200319>
- [3] Barak, M. S., Poonia, R., Devi, S., & Dhankhar, P. (2024). Nonlocal and dual-phase-lag effects in a transversely isotropic exponentially graded thermoelastic medium with voids. *ZAMM-journal of applied mathematics and mechanics/zeitschrift für angewandte mathematik und mechanik*, 104(5), e202300579. <https://doi.org/10.1002/zamm.202300579>
- [4] Singh, B. (2017). Reflection of elastic waves from plane surface of a half-space with impedance boundary conditions. *Geosciences research*, 2(4), 242–253. <https://dx.doi.org/10.22606/gr.2017.24004>

- [5] Asano, S. (1966). Reflection and refraction of elastic waves at a corrugated interface. *Bulletin of the seismological society of america*, 56(1), 201–221. <https://doi.org/10.1785/BSSA0560010201>
- [6] Singh, S. S., & Tomar, S. K. (2008). qP-wave at a corrugated interface between two dissimilar pre-stressed elastic half-spaces. *Journal of sound and vibration*, 317(3–5), 687–708. <https://doi.org/10.1016/j.jsv.2008.03.036>
- [7] Singh, A. K., Das, A., Kumar, S., & Chattopadhyay, A. (2015). Influence of corrugated boundary surfaces, reinforcement, hydrostatic stress, heterogeneity and anisotropy on Love-type wave propagation. *Meccanica*, 50(12), 2977–2994. <https://doi.org/10.1007/s11012-015-0172-6>
- [8] Singh, A. K., Mistri, K. C., & Pal, M. K. (2018). Effect of loose bonding and corrugated boundary surface on propagation of Rayleigh-type wave. *Latin american journal of solids and structures*, 15(1), e01. <https://doi.org/10.1590/1679-78253577>
- [9] Das, S. C., Acharya, D. P., & Sengupta, P. R. (1992). Surface waves in an inhomogeneous elastic medium under the influence of gravity. *Applied mechanics series*, 37(5), 539–551. <https://pascal-francis.inist.fr/vibad/index.php?action=getRecordDetail&idt=4902394>
- [10] Abd-Alla, A. M., Abo-Dahab, S. M., & Alotaibi, H. A. (2016). Effect of the rotation on a non-homogeneous infinite elastic cylinder of orthotropic material with magnetic field. *Journal of computational and theoretical nanoscience*, 13(7), 4476–4492. <https://doi.org/10.1166/jctn.2016.5308>
- [11] Chattopadhyay, A. (1975). On the dispersion equation for love waves due to irregularity in the thickness of the non-homogeneous crustal layer. *Acta geologica polonica*, 23, 307–317. <http://pascal-francis.inist.fr/vibad/index.php?action=getRecordDetail&idt=PASCALGEODEBRGM7730291681>
- [12] Roy, I., Acharya, D. P., & Acharya, S. (2017). Propagation and reflection of plane waves in a rotating magneto-elastic fibre-reinforced semi space with surface stress. *Mechanics and mechanical engineering*, 21(4), 1043–1061. <https://doi.org/10.2478/mme-2018-0074>
- [13] Singh, B., & Sindhu, R. (2011). Propagation of waves at an Interface between a liquid half-space and an orthotropic micropolar solid half-space. *Advances in acoustics and vibration*, 2011(1), 159437. <https://doi.org/10.1155/2011/159437>
- [14] Gupta, R. R., & Gupta, R. R. (2014). Surface wave characteristics in a micropolar transversely isotropic halfspace underlying an inviscid liquid layer. *International journal of applied mechanics and engineering*, 19(1), 49–60. [10.2478/ijame-2014-0005](https://doi.org/10.2478/ijame-2014-0005)
- [15] Anya, A. I., Akhtar, M. W., Abo-Dahab, S. M., Kaneez, H., Khan, A., & Jahangir, A. (2018). Effects of a magnetic field and initial stress on reflection of SV-waves at a free surface with voids under gravity. *Journal of the mechanical behavior of materials*, 27(5–6), 20180002. [doi/10.1515/jmbm-2018-0002/html](https://doi.org/10.1515/jmbm-2018-0002/html)
- [16] Anya, A. I., & Khan, A. (2019). Reflection and propagation of plane waves at free surfaces of a rotating micropolar fibre-reinforced medium with voids. *Geomechanics & engineering*, 18(6), 605–614. <https://doi.org/10.12989/gae.2019.18.6.605>
- [17] Anya, A. I., & Khan, A. (2020). Reflection and propagation of magneto-thermoelastic plane waves at free surfaces of a rotating micropolar fibre-reinforced medium under GL theory. *International journal of acoustics and vibration*, 25(2), 190–199. <https://doi.org/10.20855/ijav.2020.25.21575>
- [18] Anya, A. I., & Khan, A. (2022). Plane waves in a micropolar fibre-reinforced solid and liquid interface for non-insulated boundary under magneto-thermo-elasticity. *Journal of computational applied mechanics*, 53(2), 204–218. <https://doi.org/10.22059/jcamech.2022.341656.712>
- [19] Maleki, J., & Jafarzadeh, F. (In Press). Model tests on determining the effect of various geometrical aspects on horizontal impedance function of surface footings. *Scientia iranica*. <https://doi.org/10.24200/sci.2023.59744.6403>
- [20] Chowdhury, S., Kundu, S., Alam, P., & Gupta, S. (2021). Dispersion of stoneley waves through the irregular common interface of two hydrostatic stressed MTI media. *Scientia iranica*, 28(2), 837–846. <https://doi.org/10.24200/sci.2020.52653.2820>
- [21] Singh, B., & Kaur, B. (2022). Rayleigh surface wave at an impedance boundary of an incompressible micropolar solid half-space. *Mechanics of advanced materials and structures*, 29(25), 3942–3949. <https://doi.org/10.1080/15376494.2021.1914795>

- [22] Singh, B., & Kaur, B. (2020). Rayleigh-type surface wave on a rotating orthotropic elastic half-space with impedance boundary conditions. *Journal of vibration and control*, 26(21–22), 1980–1987. <https://doi.org/10.1177/1077546320909972>
- [23] Sahu, S. A., Mondal, S., & Nirwal, S. (2023). Mathematical analysis of rayleigh waves at the nonplanar boundary between orthotropic and micropolar media. *International journal of geomechanics*, 23(3), 4022313. <https://doi.org/10.1061/IJGNAI.GMENG-7246>
- [24] Giovannini, L. (2022). Theory of dipole-exchange spin-wave propagation in periodically corrugated films. *Physical review b*, 105(21), 214426. <https://doi.org/10.1103/PhysRevB.105.214426>
- [25] Rakshit, S., Mistri, K. C., Das, A., & Lakshman, A. (2022). Effect of interfacial imperfections on SH-wave propagation in a porous piezoelectric composite. *Mechanics of advanced materials and structures*, 29(25), 4008–4018. <https://doi.org/10.1080/15376494.2021.1916138>
- [26] Rakshit, S., Mistri, K. C., Das, A., & Lakshman, A. (2022). Stress analysis on the irregular surface of viscoporous piezoelectric half-space subjected to a moving load. *Journal of intelligent material systems and structures*, 33(10), 1244–1270. <https://doi.org/10.1177/1045389X211048226>
- [27] Eringen, A. C. (1972). Linear theory of nonlocal elasticity and dispersion of plane waves. *International journal of engineering science*, 10(5), 425–435. [https://doi.org/10.1016/0020-7225\(72\)90050-X](https://doi.org/10.1016/0020-7225(72)90050-X)
- [28] Eringen, A. C., & Wegner, J. L. (2003). *Nonlocal continuum field theories*. American society of mechanical engineers digital collection. <https://doi.org/10.1115/1.1553434>
- [29] Roy, I., Acharya, D. P., & Acharya, S. (2015). Rayleigh wave in a rotating nonlocal magnetoelastic half-plane. *Journal of theoretical and applied mechanics*, 45(4), 61. <https://doi.org/10.1515/jtam-2015-0024>
- [30] Said, S. M., Abd-Elaziz, E. M., & Othman, M. I. A. (2022). The effect of initial stress and rotation on a nonlocal fiber-reinforced thermoelastic medium with a fractional derivative heat transfer. *ZAMM - Journal of applied mathematics and mechanics*, 102(1), e202100110. <https://doi.org/10.1002/zamm.202100110>
- [31] Anya, A. I., Nwachima, C., & Ali, H. (2023). Magnetic effects on surface waves in a rotating non-homogeneous half-space with grooved and impedance boundary characteristics. *International journal of applied mechanics and engineering*, 28(4), 26–42. <https://doi.org/10.59441/ijame/172634%0D>
- [32] Anya, A. I., & Khan, A. (2019). Propagation and reflection of magneto-elastic plane waves at the free surface of a rotating micropolar fibre-reinforced medium with voids. *Journal of theoretical and applied mechanics*, 57(4), 869–881. <https://doi.org/10.15632/jtam-pl/112066%0D>
- [33] Khan, A., Anya, A. I., & Kaneez, H. (2015). Gravitational effects on surface waves in non-homogeneous rotating fibre-reinforced anisotropic elastic media with voids. *International journal of applied science and engineering research*, 4(5), 620–632. <https://www.researchgate.net/publication/343628158>
- [34] Sethi, M., Sharma, A., & Sharma, A. (2016). Propagation of SH waves in a double non-homogeneous crustal layers of finite depth lying over an homogeneous half-space. *Latin american journal of solids and structures*, 13(14), 2628–2642. <https://doi.org/10.1590/1679-78253005>
- [35] Azhar, E., Ali, H., Jahangir, A., & Anya, A. I. (2023). Effect of hall current on reflection phenomenon of magneto-thermoelastic waves in a non-local semiconducting solid. *Waves in random and complex media*, 1–18. <https://doi.org/10.1080/17455030.2023.2182146>
- [36] Ailawalia, P., Sachdeva, S. K., & Pathania, D. (2015). A two dimensional fibre reinforced micropolar thermoelastic problem for a half-space subjected to mechanical force. *Theoretical and applied mechanics*, 42(1), 11–25. <https://doi.org/10.2298/TAM1501011A>
- [37] Othman, M. I. A., Said, S. M., & Gamal, E. M. (2024). A new model of rotating nonlocal fiber-reinforced visco-thermoelastic solid using a modified Green-Lindsay theory. *Acta mechanica*, 235(5), 3167–3180. <https://doi.org/10.1007/s00707-024-03874-6%0A%0A>

Appendix

$$q_{11} = Q_{13} Q_{15};$$

$$q_{12} = -m(Q_{15} Q_{24} + Q_{13} Q_{27});$$

$$q_{13} = (-b^2 i^2 \rho Q_{12}^2 - b^2 \rho Q_{15} - \rho \omega^2 Q_{15} +$$

$$m^2 \rho Q_{24} Q_{27} - \omega^2 Q_{15} H_0^2 \varepsilon_0 \mu_0^2 +$$

$$Q_{13} (-\rho \omega^2 - b^2 \rho Q_{13} - \omega^2 H_0^2 \mu_0^2)) / \rho;$$

$$q_{14} = (m(b^2 i^2 \rho Q_{12} Q_{26} + Q_{24} (\rho \omega^2 + b^2 i^2 \rho Q_{12}$$

$$+ b^2 \rho Q_{13} + \omega^2 H_0^2 \mu_0^2) + Q_{27} \left(\rho (b^2 + \omega^2) + \omega^2 H_0^2 \varepsilon_0 \mu_0^2 \right)) / \rho;$$

$$q_{15} = \frac{1}{\rho^2} (b^2 \rho^2 \omega^2 + \rho^2 \omega^4 +$$

$$\text{bim} \rho^2 Q_{24} (-\text{bim} Q_{26}) + b^2 \rho \omega^2 H_0^2 \mu_0^2 + \rho \omega^4 H_0^2 \mu_0^2 + \rho \omega^4 H_0^2 \varepsilon_0 \mu_0^2$$

$$+ \omega^4 H_0^4 \varepsilon_0 \mu_0^4 + b^2 \rho Q_{13} (\rho (b^2 + \omega^2) + \omega^2 H_0^2 \varepsilon_0 \mu_0^2)).$$